Int. J. Electrochem. Sci., 12 **(2017)** 9601 – 9618, doi: 10.20964/2017.10.56

International Journal of
ELECTROCHEMICAL
SCIENCE
www.electrochemsci.org

Adsorption Studies and Selective Determination of Epinephrine at Glycerol-Clay Modified Glassy Carbon Electrode

Augustine O. Agyeman

Department of Chemistry and Physics, Clayton State University, 2000 Clayton State Blvd
Morrow, GA 30260
E-mail: aagyeman@clayton.edu

Received: 20 June 2017 / *Accepted:* 9 August 2017 / *Published:* 12 September 2017

Cyclic voltammetry (CV) was employed to conduct continuous repetitive scans of epinephrine (EP) at glassy carbon electrode coated with a mixture of glycerol and Standard Wyoming montmorillonite clay (SWy-2). The glycerol-clay modified electrode (GCME) was used to monitor the interfacial behavior and adsorption properties of EP and its oxidation product, adrenochrome. The clay film catalyzed EP oxidation and greatly enhanced the generation, accumulation, and adsorption of adrenochrome, without compromising system sensitivity. Progressive adsorptive accumulation was observed during repetitive scanning and maximum adsorptive accumulation (MAA) was achieved only when system pH was 7.4. A linear response was obtained in the range of 0.2 μM to 75.0 μM, with detection limit of 0.1 μM (S/N = 7). The surface coverage of the adsorbed species exhibited linear relationship with the bulk concentration, in accordance with the Langmuir isotherm. The adsorption coefficient obtained from the Langmuir isotherm was 41.3 L/g. The enhanced adrenochrome reduction peak was utilized as a simple and unique approach for selective determination of EP in the presence of serotonin, ascorbic acid, and uric acid.

Keywords: Montmorillonite clay, epinephrine, adrenochrome, adsorption, cyclic voltammetry

1. INTRODUCTION

Standard Wyoming montmorillonite (SWy-2) is a type of clay that demonstrates good electrochemical properties and has the ability to form membrane-like films. It also has high thermal stability and exhibits high resistance to extreme conditions. SWy-2 clay film on an electrode surface has the ability to increase sensitivity, selectivity, and electron transfer rate due to the unique size, shape, and layer charge [1-4]. The high surface area of clay particles [1, 5] also allows for higher adsorption of molecules. Glycerol is a chemical that is very stable, inert, and nonvolatile. Extremely

strong interactions result when glycerol intercalates into clay [6].

Epinephrine (EP), commonly called adrenaline, is one of the very important monoamine neurotransmitters in the central nervous system (CNS) of mammals. EP is involved in a variety of mental disorders and low levels have been found in patients with Parkinson's disease [7, 8]. EP is also used widely as a drug for heart surgeries, for serious allergic reactions, and under emergency medical situations [9, 10]. Analysis of EP is, therefore, essential for nerve physiology and for the development of EP medications. Many methods have been reported for the determination of EP, such as fluorescence, chemiluminescence, liquid chromatography, and capillary electrophoresis [11-14]. However, most of these methods are time consuming, complicated, and have low sensitivity, because they require derivatization or a combination of various detection techniques.

Many of the chemical processes performed by EP in the CNS are considered to be organic electrochemical processes. [15, 16]. Current methods, therefore, focus on electrochemical detection because of cost, simplicity, high sensitivity, and high accuracy [8, 17-27]. Electrochemical oxidation of EP to quinone has been studied and reports show that its electron transfer rate is slow so is often adsorbed to the electrode surface and causes passivation [21, 23-25, 28-30]. Other disadvantages of EP detection are overpotential and poor selectivity. [21, 31, 32].

However, none of the published studies focused on the interfacial behavior and adsorption properties of EP. A study of the adsorption processes of EP at electrode surfaces is of great importance to biological, biochemical, and pharmacological research, as well as the development of EP medications. Such a study would also reveal a host of potential applications in catalytic decomposition of various pharmaceutical pollutants, selective analysis of biological fluids, wastewater treatment, and gel sensor systems.

The adsorption phenomena can be complex due to the heterogeneous nature of the electrode-solution interface [33]. The strength of interaction between the surface sites and the adsorbing species may be unevenly distributed across the electrode surface. Modification of the electrode surface with the clay film is believed to generate a more homogeneous interface, improving electrochemical behavior of EP. Glassy carbon is an inert electrode and has low electrode fouling so is expected to be able to overcome any adsorption problems when coated with an appropriate membrane such as the clay film [34].

Catechol and Catecholamines readily adsorb onto metal oxide and clay minerals, with increasing surface coverage as pH increases [15, 35, 36]. SWy-2 is an Fe-bearing smectite clay mineral that contains about 2.3 mass percent lattice Fe (0.41 mol Fe/ g clay), hence strong interaction between EP and structural Fe^{3+} in the clay interlayers is expected [37, 38].

The objective of this study was to explore the various factors that affect EP adsorption at electrodes, using glycerol-clay modified glassy carbon electrode (GCME). The oxidation of EP as well as the accumulation, adsorption, and reduction of adrenochrome (EP's oxidation product) were monitored through continuous repetitive cyclic voltammetric scanning. It was observed that the GCME effectively catalyzed the oxidation of EP and facilitated the accumulation and adsorption of adrenochrome. Progressive accumulation was also observed during repetitive scanning. System equilibrium and maximum adsorptive accumulation (MAA) were achieved only at the physiological pH (7.4). The system also obeyed the Langmuir isotherm.

Further, the enhanced adsorption of adrenochrome, and hence increased reduction peak, was utilized for the selective determination of EP in the presence of serotonin (5-HT), excess ascorbic acid (AA), and excess uric acid (UA). EP coexists in biological fluids with 5-HT, AA, and UA, all of which have similar oxidation potentials. Various materials have been used to modify electrodes for selective detection or co-detection of EP, 5-HT, AA, and UA. [7-10, 15, 39-42]. However, these modified electrodes suppress adsorption and only make use of the oxidation potential, which is usually challenging. The present method is unique in the sense that the GCME rather enhances preferential adsorption and EP is determined using the increased reduction peak, which belongs to only EP.

2. EXPERIMENTAL

2.1 Chemicals and Clay

Glycerol (Mallinckrodt Chemical Works), Epinephrine (Acros Organics), Ascorbic acid (Sigma-Aldrich), serotonin (Alfa Aesar), uric acid (MP Biochemicals), sodium phosphate monobasic (Acros Organics), and sodium phosphate dibasic (Fisher Scientific), were used as received. SWy-2 clay was obtained from the Source Clay Minerals Repository (Purdue University, East Lafayette, Indiana) and processed as described below. All chemicals and clays were prepared without further purification with 18 $m\Omega.cm^3$ nanopure deionized water (Barnsted Easypure II, Thermo Scientific).

2.2 Clay Suspension

For every 15 g of the powdered clay, 500 mL of deionized water was added and stirred periodically for about 48 hours. The suspension was centrifuged at 5000 rpm (3214 rcf) for 30 minutes, using Eppendorf 5810R centrifuge. The supernatant was decanted and centrifuged again for 10 minutes. This process was repeated until no more clay particles settled at the bottom of the centrifuge tubes. The concentration of the resulting clay suspension was 7.61 mg/mL, as determined by gravimetric analysis. The clay particle size of the suspension was less than 0.2 μm, as described elsewhere [4].

2.3 Modified Electrodes

Clay suspension and glycerol (99% pure) were mixed in the ratio 95:5 by volume, unless otherwise stated. The mixtures were sonicated for two hours, using Cole-Parmer Ultrasonic Bath, and left to stand for at least twenty four hours to achieve homogeneity. With the aid of a microliter syringe, 5 μL of the glycerol-clay mixture was smeared uniformly on a polished glassy carbon working electrode and left overnight to air dry (referred to as GCME).

2.4 Phosphate Buffer Solution (PBS)

All solutions were prepared with 0.1 M phosphate buffer solution (PBS; NaH_2PO_4/Na_2HPO_4) in order to maintain solution pH of 7.40, unless otherwise stated.

2.5 Fourier Transform Infrared (FTIR) Microscopy

The Perkin Elmer Spotlight 200i FTIR Microscopy System was used for simultaneous imaging and acquisition of IR spectra. Liquid nitrogen was used to maintain low and constant detector temperature, ensuring high quality and reproducible results. GCME films were prepared on FTIR base microscope slides and air-dried overnight. With each slide on the microscope stage of the system, images (400 µm x 400 µm) and IR spectra in the micro-ATR mode were obtained simultaneously. The ATR crystal was set at a contact pressure of 5%.

2.6 Electrochemical Measurements

Cyclic voltammetry was performed using CHI 660 D potentiostat (CH Instruments, New Jersey), with the working bare electrode (BE) or GCME, an Ag/AgCl reference electrode, and a Pt counter electrode. Unless otherwise stated, the switching potentials were -0.6 V and 0.6 V, at 50 mV/s scan rate. The potentiostat was set at a sensitivity scale (A/V) of 1×10^{-6} and a quiet time of 2 seconds. The electrochemical cell was a 10-mL glass cell fitted with a 3-hole Teflon cap. All solutions were nitrogen purged (deoxygenated) for at least 10 minutes to eliminate oxygen interference and prevent the formation of oxide layer on the electrode surface. After each measurement (or set of measurements), the working electrode was polished using 0.05 micron alumina powder with polishing pad (CH Instruments) and sonicated using Cole-Parmer Ultrasonic Bath. In the case of BE, electrode was polished before and after electrochemical scans.

3. RESULTS AND DISCUSSION

3.1 Characterization of GCME by FTIR Microscopy

Glycerol was added to the clay suspension with the aim to prevent the formation of cracks in the GCME during drying. Glycerol is inert, nonvolatile, and does not alter the clay film features. Different amounts of glycerol, %(v/v) were added and examined. It was observed that 5%(v/v) glycerol produced the highest signal (not shown). Hence clay suspension used to prepare GCME contained 5%(v/v) glycerol.

The FTIR microscope system was used to examine the morphological features of the GCME as shown in Figure 1. High quality films were obtained as confirmed by FTIR microscopy. Figure 1A shows the IR micro-ATR spectra of glycerol, clay and glycerol-clay mixture. It can be seen that both glycerol and clay have similar characteristic bands at similar wavenumbers. The SWy-2 clay is a

hydrous aluminosilicate layered material that consists of structural OH groups, tetrahedral silicates (Si-O), and octahedral aluminates (Al-O and Al-OH) [3, 4]. The broad band centered around 3300 cm^{-1} is due to hydrogen bonding of the structural OH groups in the clay (also OH of glycerol). The weak band around 2900 cm^{-1} is a result of Si-H bond (C-H bond of glycerol where the C is sp^3 hybridized). In addition, Si=O stretching band was observed at 1630 cm^{-1}. The strong stretching band at 1040 cm^{-1} is a result of Si-O stretch from the silicates (C-O stretch from glycerol). It could also come from Al-O stretch. It can be seen from the glycerol-clay spectrum that the addition of glycerol did not cause significant changes in the bands. Only slight shifts were observed due to interactions of glycerol with the clay.

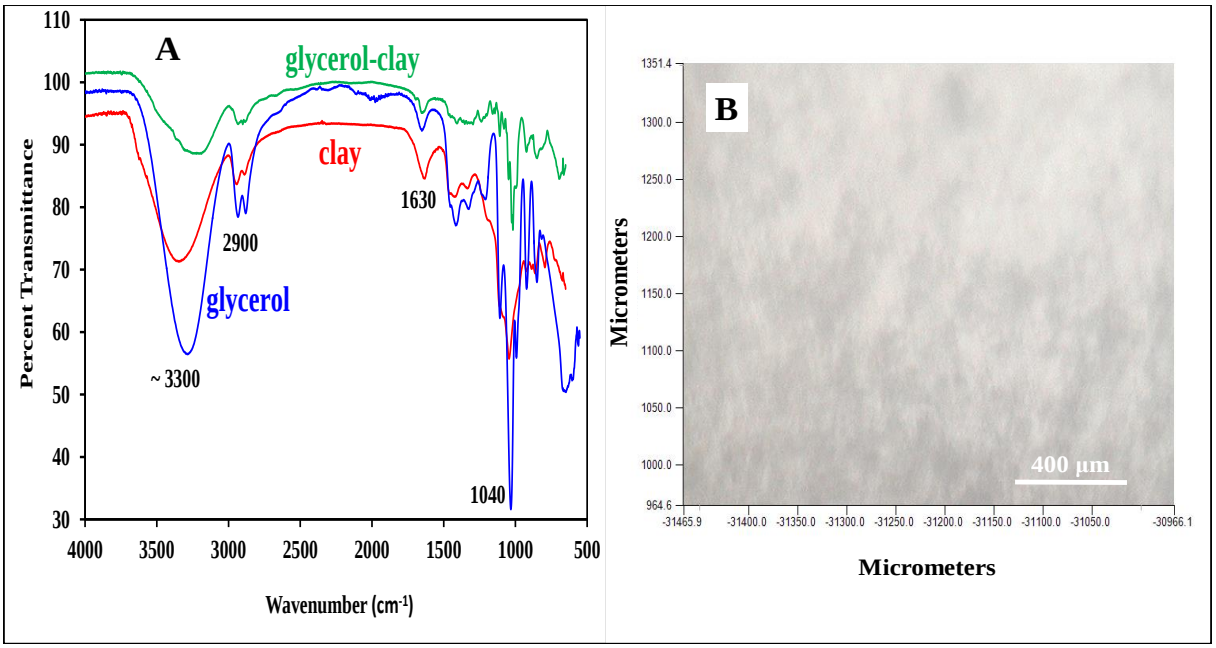

Figure 1. (A) FTIR microscopy spectrum for clay and glycerol-clay films in the ATR mode; (B) FTIR microscopy image of glycerol-clay film.

3.2 EP Adsorption Studies at BE

The interfacial behavior of EP at bare glassy carbon electrode (BE) was evaluated. Figure 2A illustrates ten cycles of repetitive cyclic voltammogram (CV) at BE, for 50.0 µM EP in 0.10 M PBS (pH 7.4). The potential was scanned between -0.6 V and 0.6 V (vs Ag/AgCl) at a scan rate of 50 mV/s. The first cycle showed an oxidative peak "a" ($i_{p,a}$) around 0.28 V and a reductive peak "b" ($i_{p,b}$) around -0.19 V. An oxidative peak "c" ($i_{p,c}$) around -0.14 V appeared during the second cycle. The $i_{p,a}$ decreased substantially with subsequent cycles whilst $i_{p,b}$ and $i_{p,c}$ increased gradually. This is an indication of progressive adsorptive accumulation at the electrode surface.

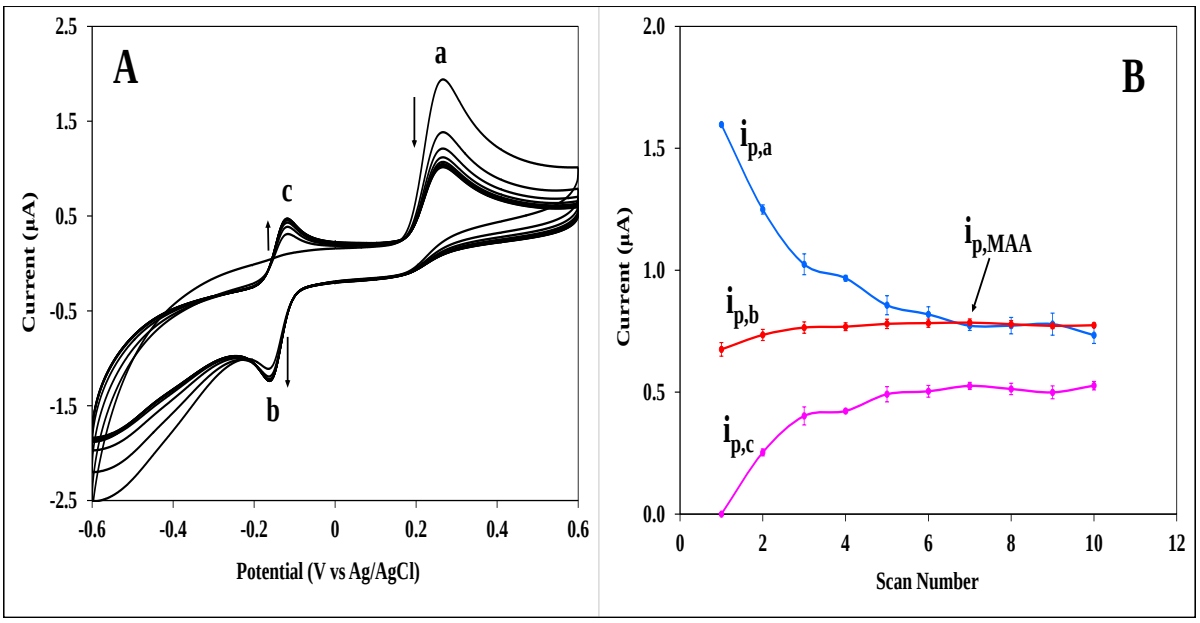

Figure 2. (A) Cyclic voltammogram of continuous repetitive scanning at 50 mV/s for 50.0 µM EP in 0.1 M PBS (pH 7.4) at BE; (B) A plot of peak currents "a" ($i_{p,a}$), "b" ($i_{p,b}$), and "c" ($i_{p,c}$) versus scan number.

EP was first oxidized to its open chain quinone, corresponding to $i_{p,a}$, with the loss of two electrons and two protons [28, 41-44]. The electrochemical oxidation of EP takes place at the phenol groups of the molecule to form the homologue quinone (peak "a"). This oxidation product is very unstable, hence the absence of a corresponding reduction peak. The quinone underwent intramolecular cyclization (via nucleophilic attack by the nitrogen), followed by aromatization (via proton transfer) to generate the inetermediate, leucochrome, and then adrenochrome as the final oxidation product [43]. The adrenochrome product then adsorbed to the electrode surface and passivated the electrode over time, which is the reason why $i_{p,a}$ reduced with subsequent cycles. This implies that the adsorption of adrenochrome was very strong and interfered with the electrochemical detection of EP. Adrenochrome underwent electrochemical reduction to form leucochrome, corresponding to $i_{p,b}$, which then reoxidized back to adrenochrome, corresponding to $i_{p,c}$ [23, 24, 28, 41]. This explains why $i_{p,c}$ was absent in the first cycle as there was no adrenochrome to convert electrochemically to leucochrome. Therefore, $i_{p,b}$ and $i_{p,c}$, centered at -0.17 V, were attributed to the redox couple, adrenochrone/leucochrome.

The oxidation of EP to adrenochrome has been studied extensively [43, 44]. Garnayak and Patel reported that the quinone intermediate has a half-life of only about 0.06 s, which implies the conversion between quinone and adrenochrome is very fast [43]. At a scan rate of 50 mV/s, it takes about 18 seconds to move from $i_{p,a}$ to peak $i_{p,b}$, which is quite an ample time for the intramolecular conversion to adrenochrome to take place. Karin et. al. proposed that the oxidation product of catecholamines must be adsorbed onto the electrode surface in order for the second oxidation ($i_{p,c}$ in this case) to be observed [26]. Their proposal is in agreement with the above observation as $i_{p,c}$ was absent during the first cycle. They also reported that catecholamines adsorb to the surface with the

aromatic ring oriented parallel to the electrode surface, and with the positively charged amine end of the molecule held away from the electrode surface. This allows the catecholamine to oxidize to quinone, undergo any intramolecular changes, adsorb, and then reorient in such a way that the amine becomes accessible to the electrode surface. This is also consistent with the above observations of $i_{p,b}$ and $i_{p,c}$ being attributed to the adrenochrome/luecochrome redox couple.

Negligible shift in the peak potentials were observed with subsequent cycles at all three peaks. On the average, the peak separation (ΔE_p) between $i_{p,b}$ and $i_{p,c}$ was about 50 mV, which remained fairly constant with subsequent cycles. This is a characteristic of 2-electron processes of an adsorbed species [34].

Figure 2B depicts the relationships between the peak currents and scan number during the repetitive scans (results are averages of 3 independent scans). At the seventh cycle, $i_{p,a}$ minimized and leveled off afterwards, while $i_{p,b}$ and $i_{p,c}$ maximized and plateaued, indicating the occurrence of maximum adsorptive accumulation (MAA). Also at the seventh cycle, $i_{p,a} \approx i_{p,b}$ (denoted $i_{p,MAA}$). That is, lines "a" and "b" coincided, which indicated the establishment of equilibrium. Hence, both equilibration and MAA occurred simultaneously, at the seventh cycle.

Equation 1 below can be used to calculate the surface coverage (Γ) at system equilibrium and MAA, using $i_{p,MAA}$ from the seventh cycle [45]:

$$\Gamma = Q/nFA \quad (1)$$

where Q is the quantity of charge consumed during reduction or adsorption (0.608 C), n is the number of electrons transferred (2 electrons), F is Faraday constant (9.6485×10^4 C/mol), and A is the electrode area (0.0707 cm^2). The charge in coulombs (C), was obtained by integrating the area under the voltammetric peak. This resulted in a surface coverage of 44.6 pmol/cm^2 at MAA with bulk concentration (C_b) of 50.0 μM.

Immediately after the repetitive scans, the electrode was transferred to 0.1 M PBS solution and similar repetitive scans were acquired. All three peaks were present, which confirmed adsorption of EP and its oxidation products (not shown). All the peaks decreased with subsequent scans, with $i_{p,a}$ completely disappearing after the seventh cycle. It is interesting to note that equilibration and MAA occurred at the seventh cycle while it took seven cycles for $i_{p,a}$ to completely disappear during desorption in PBS. On the other hand, $i_{p,b}$ and $i_{p,c}$ did not disappear completely, even after several cycles. This suggested that adsorption of adrenochrome to the carbon electrode was very strong.

In addition, BE was scanned in 50.0 μM EP using -0.6 V and 0 V as the switching potentials. No peaks were observed after ten repetitive scans. Within these potentials, EP could not oxidize to quinone, hence production and adsorption of adrenochrome did not occur.

3.3 EP Adsorption Studies at GCME

The interfacial behavior of EP at GCME was similarly evaluated using the same parameters as in section 3.2 above. Figure 3A shows ten repetitive cyclic voltammograms at GCME for 50.0 μM EP in 0.10 M PBS (pH 7.4). The first cycle exhibited both the oxidative $i_{p,a}$ and $i_{p,c}$, as well as the reductive $i_{p,b}$. Peak potentials for $i_{p,a}$, $i_{p,b}$, and $i_{p,c}$, were around 0.29 V, -0.17 V, and -0.12 V,

respectively. Compared to BE, $i_{p,a}$ shifted more positive by 10 mV while $i_{p,b}$ and $i_{p,c}$ shifted more positive by 20 mV each. The difference in potentials between $i_{p,a}$ and $i_{p,b}$ reduced by 10 mV, which may be due to increased adsorption or faster electron-transfer kinetics [17]. The ΔE_p between $i_{p,b}$ and $i_{p,c}$ was about 50 mV (same as BE), characteristic of 2-electron processes of an adsorbed species [34]. Also, the repetitive scans did not cause any significant shift in peak potentials.

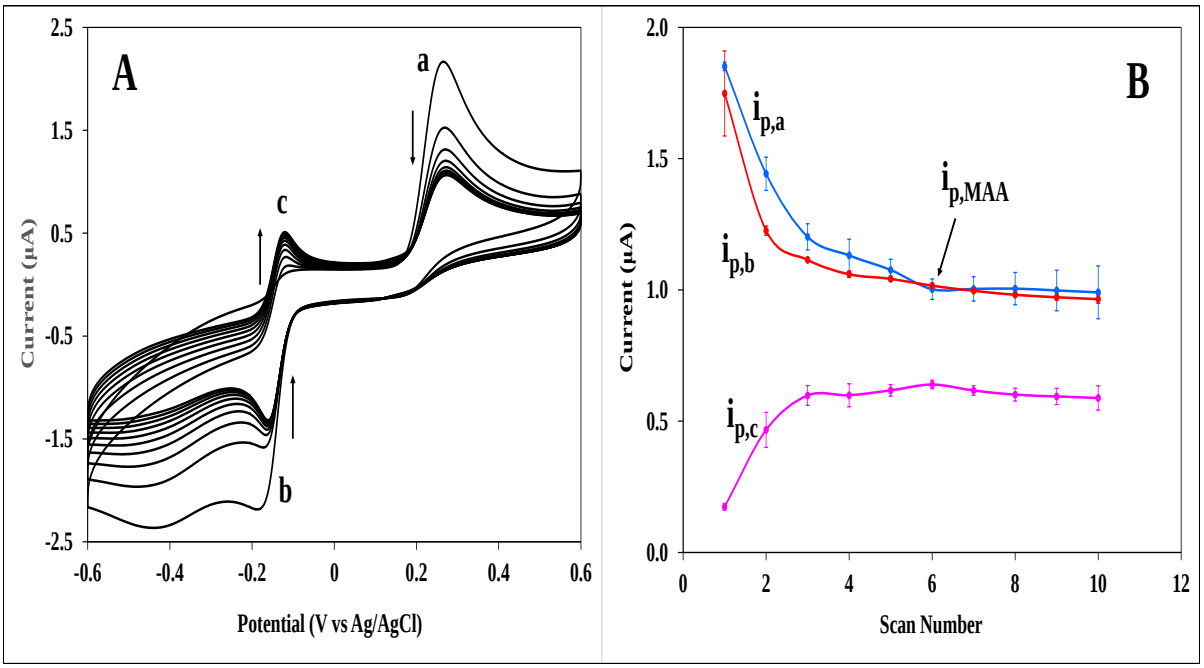

Figure 3. (A) Cyclic voltammogram of continuous repetitive scanning at 50 mV/s for 50.0 µM EP in 0.1 M PBS (pH 7.4) at GCME; (B) A plot of peak currents "a" ($i_{p,a}$), "b" ($i_{p,b}$), and "c" ($i_{p,c}$) versus scan number.

Unlike $i_{p,b}$ at BE, the $i_{p,b}$ at GCME exhibited relatively high peak current at the first cycle and was very close in magnitude to $i_{p,a}$, as shown in Figure 3B. The $i_{p,b}$ at GCME was, on the average, 2.5 times higher than that at BE. This is an indication that there was enhanced conversion from EP through adrenochrome to luecochrome. The clay film catalyzed the system and enhanced retention and adsorption of adrenochrome.

Both $i_{p,a}$ and $i_{p,b}$ decreased with subsequent cycles while $i_{p,c}$ increased gradually, indicative of progressive adsorptive accumulation at GCME. While $i_{p,a}$ at GCME was similar in magnitude to that at BE, $i_{p,b}$ and $i_{p,c}$ were relatively higher. The large surface area of clay particles resulted in an increase in electroactive surface area and adsorption sites, which increased adsorption and caused higher currents. Also, the clay film interlayers were able to trap and accumulate EP and its oxidation products, leading to high currents.

Further, $i_{p,c}$ was observed at first cycle, implying that the clay film initially catalyzed EP oxidation before potential application, consistent with the electrocatalytic effect of the clay. Hence, the clay-modified electrode exhibited enhanced adsorption kinetics without compromising sensitivity.

It can be seen from Figure 3B that $i_{p,a}$ and $i_{p,b}$ were very close in magnitude at first cycle,

separated out while decreasing, and coincided from the sixth cycle. Also at the sixth cycle, $i_{p,a}$ and $i_{p,b}$ minimized and leveled off while $i_{p,c}$ maximized. Hence, equilibration and MAA occurred at the sixth cycle, one cycle earlier than BE.

Using equation (1) in section 3.2 above, the surface coverage at MAA was determined to be 54.5 pmol/cm^2. This was about 10 pmol/cm^2 higher than that of BE, confirming enhanced adsorption at the GCME. The results show that the clay platelets of the film arrange themselves in a controllable way during drying of the film, which facilitated intercalation and increased adsorption.

Similar to BE, the GCME was immediately transferred from EP solution to PBS solution to monitor desorption. Results were similar to BE as described in section 3.2 above, only that $i_{p,a}$ completely disappeared after eight cycles. The clay film was able to retain more of the adsorbed species and for longer period of time, compared to BE.

GCME was also scanned in 50.0 µM EP using -0.6 V and 0 V as the switching potentials. Both $i_{p,b}$ and $i_{p,c}$ were present at first cycle, with reduction in $i_{p,b}$ and an increase in $i_{p,c}$ during subsequent cycles. The oxidation process was not due to potential application but the electrocatalytic activity of the clay film.

3.4 Effect of Bulk Concentration

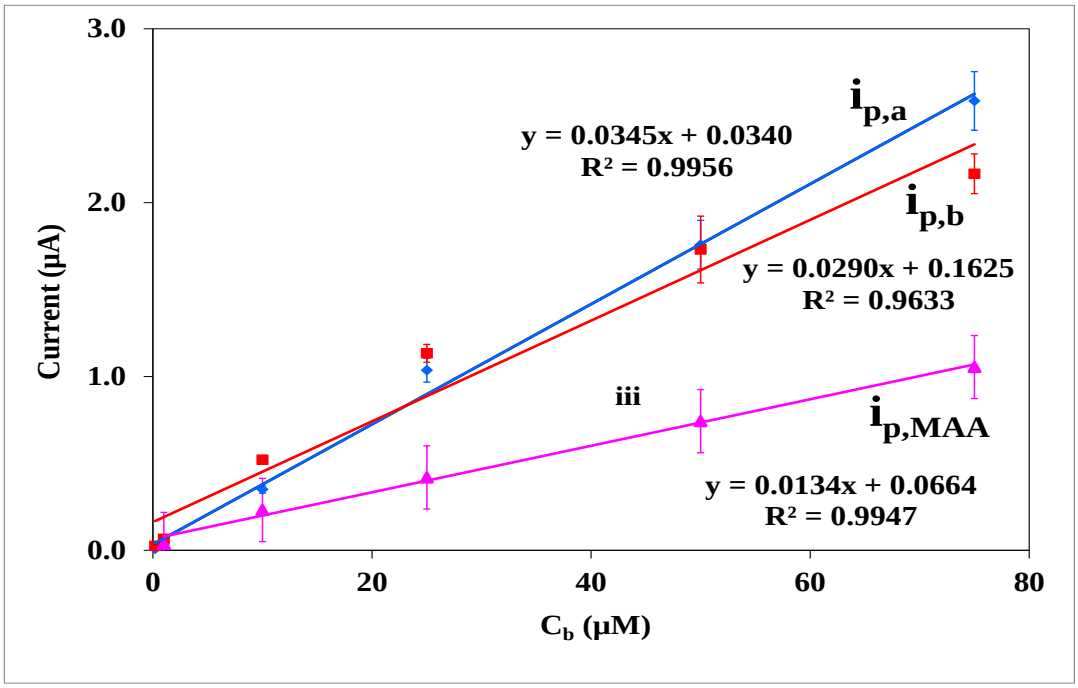

Figure 4. Calibration curves (peak current vs. bulk concentration) at 50 mV/s for EP in 0.1 M PBS (pH 7.4) at GCME ($i_{p,a}$, and $i_{p,b}$, values from the first cycle).

The effect of EP bulk concentration (C_b) on voltammetric response was investigated. Figure 4 shows calibration curves for $i_{p,a}$, $i_{p,b}$, and $i_{p,MAA}$ ($i_{p,a}$, and $i_{p,b}$, values from the first cycle). The curves $i_{p,a}$ and $i_{p,b}$ gave linear relationships within a concentration range of 0.2 µM and 75 µM, at the chosen

instrument sensitivity scale (A/V) of 1 x 10^{-6}. The limit of detection (LOD) of EP was found to be 0.1 μM (S/N = 7). The respective linear regression equations for $i_{p,a}$ and $i_{p,b}$ were $i_{p,a} = 0.0345C_b + 0.0340$ ($R^2 = 0.9956$) and $i_{p,b} = 0.0290C_b + 0.1625$ ($R^2 = 0.9633$). The coefficient of determination, R^2, in each case was very strong ($0.8 < R^2 < 1$), an indication that the peak currents are highly correlated with the concentrations. This implies that the regression models will provide highly accurate predictive concentration values.

Similarly, curve $i_{p,MAA}$ showed a linear calibration curve within a concentration range of 1.0 μM and 75.0 μM. The linear regression equation was $i_{p,MAA} = 0.0134C_b + 0.0664$ ($R^2 = 0.9947$), which also exhibited strong coefficient of determination. Equilibrium and MAA did not establish at concentrations outside this range. The system was over saturated with EP at concentrations above 75.0 μM. There were contributions from both diffusion and adsorption at higher concentrations, hence the peak currents did not completely plateau with subsequent cycles. Also, amount of adrenochrome needed to establish equilibrium could not be generated at concentrations below 1.0 μM.

The linear range and LOD of the present modified electrode was compared with those of similar modified electrodes for EP detection, as summarized in Table 1 below. It can be seen from the table that the GCME is more sensitive with lower LOD than many published reports.

Table 1. Comparison of LOD and linear range of EP at GCME with other EP electrochemical sensors.

Reference	Type of Electrode	Linear Range (μM)	LOD (μM)
This study	Glycerol-Clay Modified GCE	0.2 - 75	0.1
8	Caffeic Acid Modified GCE	2 - 300	0.6
9	Caffeic Acid Modified GCE	2 - 80	0.2
10	TTAB Modified Carbon Paste Electrode	0.15 - 2.5	0.12
15	Iron(III) Doped Zeolite-Modified Carbon Paste	0.9 - 216	0.44
24	L-Cysteine Monolayers Modified Gold Electrode	0.1 - 2	0.01
19	L-Glutamic Acid Graphene Modified Electrode	0.1 - 1000	0.03
20	Boron-Doped Diamond Film Electrode	0.7 - 60	0.21
28	Penicillamine Self-Assembled Gold Electrode	0.5 - 1 & 10 - 200	0.1
39	Poly(Eriochrome Black T) Modified GCE	2.5 - 50	0.3

3.5 Adsorption Isotherm

A plot of Γ versus C_b revealed a linear relationship within a range of 1.0 μM and 75.0 μM (Figure 5), the same concentration range within which system equilibrium and MAA were established. The values of Q corresponding to $i_{p,MAA}$ were used to calculate the Γ values. The linear regression equation was $\Gamma = 0.0010C_b + 4.8666$ ($R^2 = 0.9947$). The coefficient of determination was very strong, hence the surface coverage of adsorbed adrenochrome is highly correlated with EP bulk concentration. The linearity implies that the adsorption process obeys the Langmuir isotherm. The thermodynamic

strength of adsorption can be estimated using the slope of the linear plot of the Langmuir isotherm, according to equation (2) below [33, 45]:

$$\Gamma = \Gamma_m B C_b \quad (2)$$

where Γ_m is the surface coverage at saturation (the maximum attainable Γ) and B is the adsorption coefficient. The Langmuir model assumes that $BC_b << 1$, that there are no interactions between adsorbed species, and that there is a monolayer coverage. The slope of the curve ($\Gamma_m B$) was 1.0×10^{-3} cm. The peak currents deviated from linearity at concentrations higher than 75.0 μM and began to plateau from 100.0 μM. Using 100.0 μM EP as the saturation point, Γ_m was estimated as 132 pmol/cm^2. A value that is reasonable compared to the maximum surface coverage of 240 pmol/cm^2 obtained for the adsorption of catechol on goethite clay [35]. From the slope and Γ_m, the adsorption coefficient (B) of EP on SWy-2 clay was determined to be 41.3 L/g. This is comparable to Langmiur coefficients for adsorption of Cr(VI) on different kinds of kaolinite clays, which were within the range 29.7-39.3 L/g [46].

It must be noted that multilayer adsorption is possible (depending on experimental conditions) and cannot be detected only by surface coverage analysis [33].

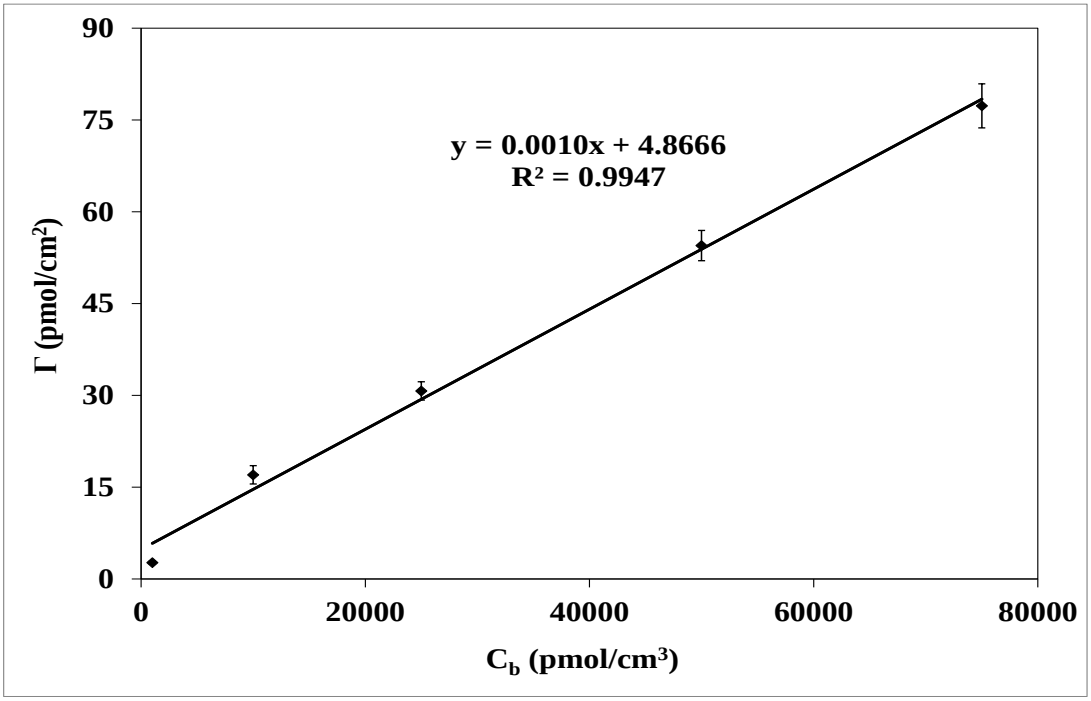

Figure 5. A plot of surface coverage (Γ, corresponding to $i_{p,MAA}$) versus bulk concentration (C_b) at 50 mV/s for EP in 0.1 M PBS (pH 7.4) at GCME.

3.6 Effect of Scan Rate

The effect of scan rate (ν) on the electrochemical behavior of EP was investigated with 50.0 μM EP in 0.10 M PBS (pH 7.4). All three peaks increased with increasing ν, but $i_{p,c}$ maximized and leveled-off at 250 mV/s. Due to that, ν values used for the investigation were ≤ 250 mV/s.

A plot of $i_{p,a}$ (μA) versus $\nu^{1/2}$ $(V/s)^{1/2}$ gave a linear relationship (not shown), indicative of diffusion-controlled process. The linear regression equation was $i_{p,a} = 6.0822\nu^{1/2} + 0.3139$ (R^2 = 0.9820). Also, a graph of log $i_{p,a}$ vs log ν was linear with a slope of 0.37 (not shown). The theoretical value (upper limit) for purely diffusion-controlled processes is 0.53, hence the linearity and slope confirmed a diffusion-controlled process [47]. Also, $i_{p,a}$ shifted slightly positive with increasing ν, indicating a quasi-reversible system [8].

On the other hand, $i_{p,b}$ and $i_{p,MAA}$ increased linearly with respect to ν, indicative of surface-controlled adsorptive processes. The respective linear regression equations were $i_{p,b} = 3.2491\nu + 0.8875$ (R^2 = 0.9753) and $i_{p,MAA} = 6.4913\nu + 0.6625$ (R^2 = 0.9829).

These results reveal that the process is simultaneously dominated by both diffusion and adsorption [47]. The system approaches ideal behavior when ν is relatively slow, when there is no intermolecular interactions of the adsorbed layer, or when fast electron transfer occurs [45].

3.7 Effect of pH

The effect of pH on EP oxidation and adsorption was investigated using the following pH values: 2.5, 4, 6, 7.4, 9, and 11. Figures 6A and 6B show the effect of pH on peak currents and potentials. It can be seen from Figure 6A that peak potentials shifted more negative with increasing pH, which showed that protons have participated in the electrode reaction processes. [8, 15]. Plots of peak potentials versus pH for $i_{p,a}$ and $i_{p,b}$ gave linear relationships with negative slopes of 67 mV/pH and 47 mV/pH, respectively (not shown).

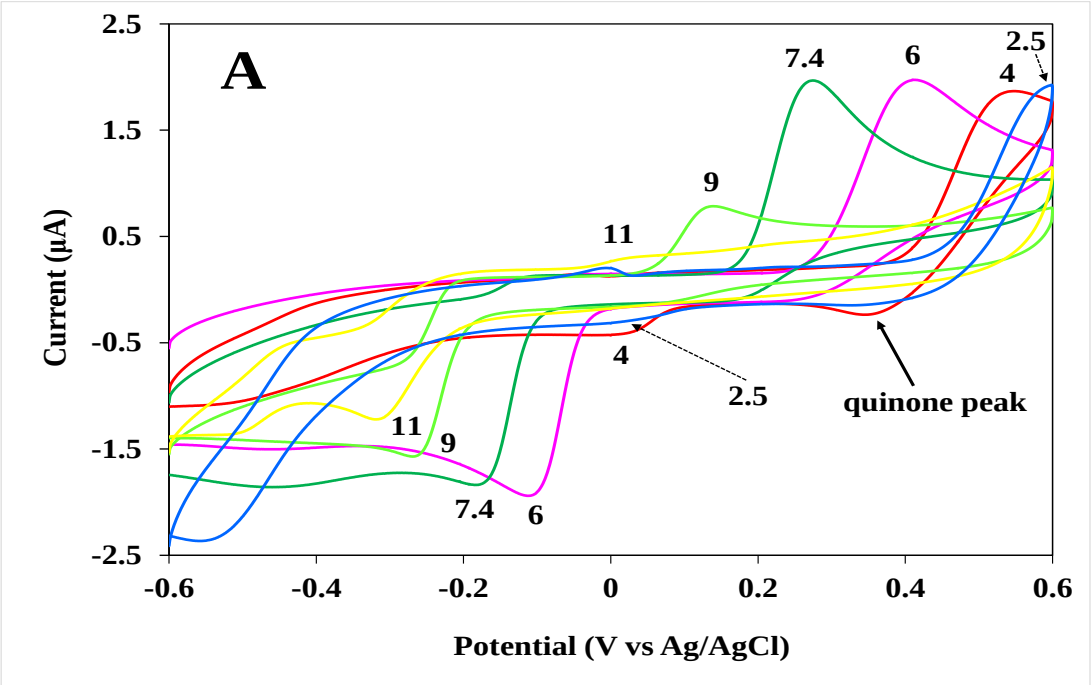

Figure 6A. Cyclic voltammograms at 50 mV/s for 50.0 μM EP at GCME at different pH values (2.5, 4, 6, 7.4, 9, and 11).

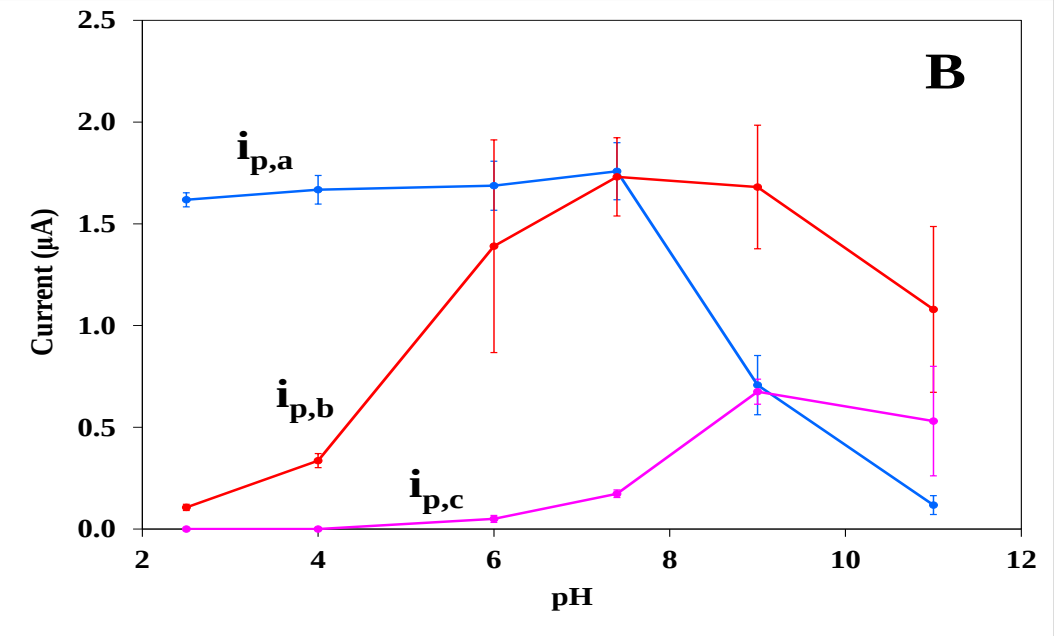

Figure 6B. A plot of peak currents "a" ($i_{p,a}$), "b" ($i_{p,b}$), and "c" ($i_{p,c}$) versus pH.

Linearity shows that the behavior obeys the Nernst equation. The slopes are close to 59 mV/pH (for an ideal Nernstian behavior), which means that the uptake of electrons is accompanied by an equal number of protons [8, 15]. It is known from section 3.2 above that EP oxidation processes involve 2 protons and 2 electrons.

Both $i_{p,a}$ and $i_{p,b}$ increased with increasing pH, reaching a maximum at pH 7.4, and decreased beyond 7.4, as shown in Figure 6B. Therefore, pH 7.4 (the physiological pH) produced the highest signal for electrochemical analysis of EP. In addition, with the exception of pH 7.4, equilibration and MAA was not established at any other pH. EP readily oxidizes upon potential application, and converts to adrenochrome at pH around 7 [44]. It can also be seen that $i_{p,a} \approx i_{p,b}$ at pH 7.4, whereas $i_{p,a} \approx i_{p,c}$ at pH 9.

At pH of 4, little return peak for $i_{p,a}$, believed to be due to quinone, was observed around 0.37 V (indicated by an arrow in Figure 6A). The characteristics of the CV in acidic medium indicated lack of adsorption of the oxidation products. The pK_a of EP is ~ 8.6 [15, 41], which means that EP exists in the cationic form in acidic medium (the nitrogen is protonated), implying the oxidized quinone is also cationic [26, 43]. Nucleophilic attack by the nitrogen is prevented due to its protonation, hence cyclization does not proceed. In addition, at very low pH values, there is believed to be competition between the protonated EP and solution protons for adsorption sites within the film and at the electrode surface. Conversely, the nitrogen (amine group) is not protonated at higher pH values and the free base readily undergoes cyclization.

In strongly alkaline medium (pH ≥ 9), $i_{p,a}$ decreased drastically due to the deprotonation of EP, reducing accumulation and adsorption into the clay film. EP readily oxidized in alkaline medium before applying potential scan, which resulted in higher $i_{p,b}$ and $i_{p,c}$, relative to $i_{p,a}$. Further, adrenochrome is unstable in alkaline medium and readily reacts with hydroxide ions [44], increasing the rate of oxidation and causing more EP to oxidize to adrenochrome in the bulk solution. The rate of

EP oxidation at pH 8 has been reported to be about four times greater than that in very acidic medium [44].

The positively charged EP at pH < 8.6 (the pK_a of EP) enhanced intercalation and accumulation within the clay interlayers, due to the net negative charge on the SWy-2 clay layers and its cation-exchange properties [48]. The clay layer edges are negatively charged at pH > 7 whereas the layer surfaces are almost always negatively charged. Since EP is positively charged at pH 7.4, it was readily attracted into the interlayers of the clay film. This enhanced adsorption and detection of EP and its oxidation products. As previously stated, the SWy-2 clay contains about 2.3 mass percent lattice Fe (0.41 mol Fe/ g clay) [37, 38], which also resulted in strong interactions between EP and structural Fe^{3+} and improved adsorption and accumulation.

3.8 Selectivity Studies

The use of modified electrodes for selective measurements of neurotransmitters has been an area of focus in electroanalytical research. The effect of 5-HT, AA, and UA on the electrochemical detection of EP was investigated. These substances are difficult to differentiate electrochemically from EP, since their oxidation peaks occur at similar potentials.

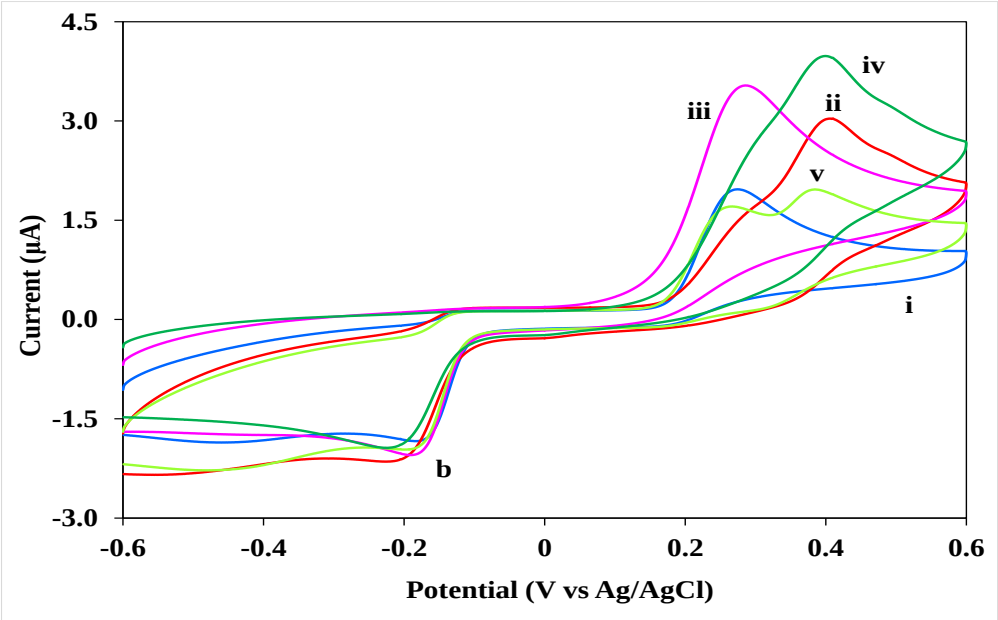

Figure 7. Cyclic voltammograms at 50 mV/s for the following mixtures in 0.1 M PBS (pH 7.4) at GCME: (i) 50.0 µM EP, (ii) 50.0 µM EP + 50.0 µM 5-HT, (iii) 50.0 µM EP + 250.0 µM AA, (iv) 50.0 µM EP + 50.0 µM 5-HT + 250.0 µM AA, and (v) 50.0 µM EP + 250.0 µM UA.

Figure 7 shows the CVs of the following species at GCME: (i) 50.0 µM EP, (ii) 50.0 µM EP + 50.0 µM 5-HT, (iii) 50.0 µM EP + 250.0 µM AA, (iv) 50.0 µM EP + 50.0 µM 5-HT + 250.0 µM AA, and (v) 50.0 µM EP + 250.0 µM UA. Excess amounts AA and UA were used since they usually exist in relatively large amounts in biological samples. It can be seen that the oxidation potentials of all the

species were very close and interfered with $i_{p,a}$ of EP. However, $i_{p,b}$ remained unaltered irrespective of the species mixed with EP, since none of them exhibits such a reduction peak. In view of this, the easiest way to discriminate between EP and the other interfering species is to monitor the adrenochrome reduction peak, $i_{p,b}$. The measured $i_{p,b}$ of all the five CVs shown in Figure 7 were within 1.731 ± 0.188 µA (mean ± standard deviation from 3 measurements of pure EP). In fact, they were all within an error of 5%, which is a highly acceptable tolerance limit for the determination of EP concentration in the presence of interfering species. The increase of $i_{p,b}$ by a factor of about 2.5 at GCME compared to BE enhances sensitivity, which offers a reliable way of selectively quantifying EP in the presence of interfering species. Recall from section 3.4 that the calibration curve for $i_{p,b}$ has strong coefficient of determination, which will provide reliable and highly accurate predictive concentration values of EP. One other noticeable advantage is the marked peak separation between EP and UA ("v" in Figure 7).

3.9. EP Determination in Urine Samples

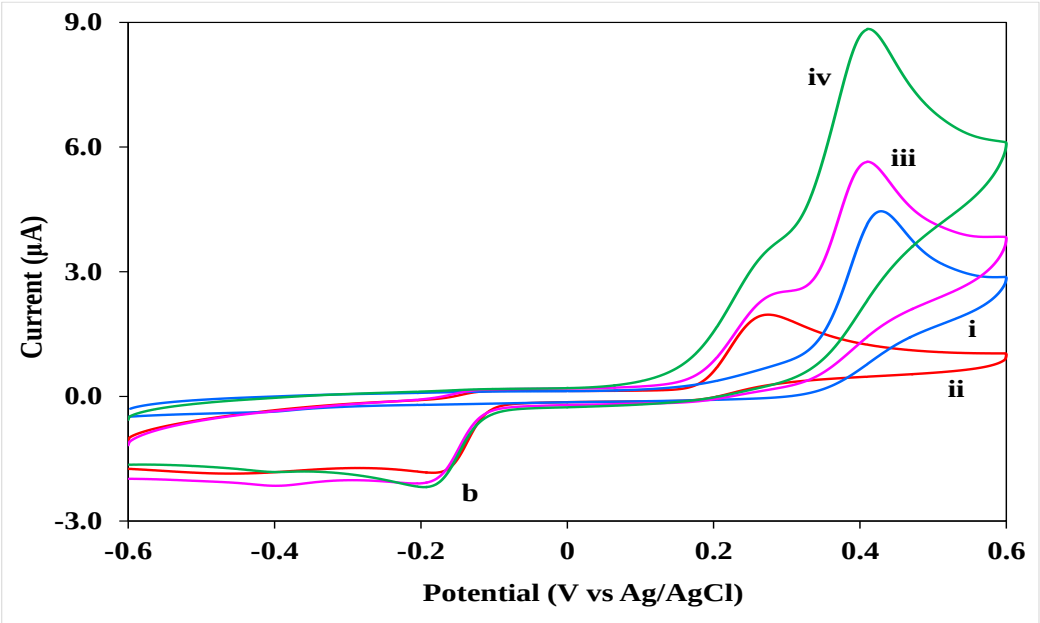

Figure 8. Cyclic voltammograms at 50 mV/s for the following urine samples (10-fold dilution with 0.1 M PBS, pH 7.4) at GCME: (i) urine, (ii) 50.0 µM EP in PBS, (iii) urine spiked with 50.0 µM EP, and (iv) urine spiked with 50.0 µM EP + 50.0 µM 5-HT + 100.0 µM AA + 100.0 µM UA.

The performance of the GCME was investigated by determining the amount of EP in urine samples as a real complex matrix, obtained from a healthy individual. Pure urine samples saturated the system and exhibited current overload at $i_{p,a}$ so samples were diluted 10-fold with 0.1 M PBS buffer.

Figure 8 shows the CVs from urine, 50.0 µM EP in PBS, urine spiked with standard 50.0 µM EP, and urine spiked with a mixture of 50.0 µM EP + 50.0 µM 5-HT + 100.0 µM AA + 100.0 µM UA. Similar to the interfering species discussed in section 3.8 above, urine exhibited oxidation peak around $i_{p,a}$, which interferes with EP determination using the oxidation potential. However, urine did not

exhibit any peak at $i_{p,b}$. Also, $i_{p,b}$ remained unaltered irrespective of the EP mixture spiked into the urine samples.

Table 2 summarizes the recovered EP amount compared with the spiked EP amount in the urine samples (average of 5 measurements). The data demonstrates good reproducibility and recovery, showing that the method can be used for the detection of trace amounts of EP in real biological samples. It can be seen that the GCME selectively and efficiently detected EP irrespective of the matrix and the interfering species present. Results were within an error of 5%, which is a highly acceptable tolerance limit for the determination of EP in the presence of interfering species.

Table 2. Determination of EP in urine (mean ± standard deviation from 5 measurements)

Sample	Determined (μM)	%RSD	% Recovery
Urine	-	-	-
Urine spiked with 50.0 μM EP	51.77 ± 1.81	3.50	103.54
Urine spiked with 50.0 μM EP, 50.0 μM 5-HT, 100.0 μM AA, 100.0 μM UA	51.75 ± 0.46	0.88	103.50

4. CONCLUSION

In this work, a simple glycerol-clay modified glassy carbon electrode (GCME) for studying the interfacial behavior and adsorption properties of EP has been introduced. The oxidation of EP, cyclization to adrenochrome, reduction of adrenochrome to leucochrome, system equilibration, and adsorptive accumulation, were monitored using cyclic voltammetry through continuous repetitive scanning. System conditions, such as glycerol-clay composition, concentration range, scan rate range, and pH were optimized. The clay film efficiently catalyzed EP oxidation and facilitated adrenochrome adsorption, without compromising sensitivity. The electrostatic attraction between the clay and EP enhanced adsorption and confinement within the film. System equilibrium and maximum adsorptive accumulation were established only at the physiological pH of 7.4. The highest sensitivity was also observed at pH 7.4. The electrocatalytic mechanism of EP was different under various pH conditions. The detection limit of EP was 0.10 μM (S/N = 7), which is lower than most published reports that use conventional electrodes. The adsorption coefficient was 41.3 L/g. The GCME provides a unique, easy, and reliable approach for selective detection of EP in the presence of serotonin, ascorbic acid, and uric acid, by monitoring the enhanced reduction peak of adrenochrome. It was demonstrated that EP has different adsorption properties from these interfering species, which resulted in preferential adsorption at the GCME. The GCME also demonstrated high selectivity and efficient recovery for EP in real urine samples. This work offers different conditions under which adsorption can be enhanced, prevented, or minimized, depending on the intended application. The system offers high sensitivity and reproducibility, with long-term stability.

ACKNOWLEDGMENTS
The author is grateful to the Undergraduate Research and Creative Activities (URCA) program and the College of Arts & Sciences Minigrant program at Clayton State University for providing research funds.

References

1. P. K. Ghosh, A. J. Bard, *J. Phys. Chem*., 88 (1984) 5519.
2. P. Subramanian, A. Fitch, *Environ. Sci. Tech*., 26 (1992) 1775.
3. A. Fitch, J. Du, *J. Electroanal. Chem. Interf. Electrochem*., 319 (1991) 409.
4. S. Macha, A. Fitch, *Mikrochim. Acta*, 128 (1998) 1.
5. R. A. Schoonheydt, P. De Pauw, D. Vliers, F. C. De Schrijver, *J. Phys. Chem*., 88 (1984) 5113.
6. Y. Xi, R. J. Davis, *Clays Clay Miner*., 58 (2010) 475.
7. B. Hadi, K.-M. Hassan, K. Hojatollah, *Anal. Chem*., 80 (2008) 9848.
8. R. Wang, Q. L. Hong, B. L. Nian, *Sensors*, 6 (2006) 80.
9. R. Wang, Q. L. Hong, B. L. Nian, *Biosens. Bioelectron*., 21 (2006) 1086.
10. S. S. Shankar, B. E. K. Swamy, *Int. J. Electrochem. Sci.*, 9 (2014) 1321.
11. Y. Guo, J. Yang, X. Wu, A. Du, *J. Fluoresc*., 15 (2005) 131.
12. Z. Guo, S. Dong, *Electroanalysis*, 17 (2005) 607.
13. M. A. Fotopoulou, P. C. Ioannou, *Anal. Chim. Acta*, 462 (2002) 179.
14. S. Wei, G. Song, J.-M. Lin, *J. Chromatogr*. A., 1098 (2005) 166.
15. A. Babaei, S. Mirzakhani, B. Khalilzadeh, *J. Braz. Chem. Soc*., 20 (2009) 1862.
16. Q. Zhao, Z. Gan, Q. Zhuang, *Electroanalysis*, 14 (2002) 1609.
17. A. G. Zestos, C. B. Jacobs, E. Trikantzopoulos, A. E. Ross, B. J. Venton, *Anal. Chem*., 86 (2014) 8568.
18. T. Thomas, R. J. Mascarenhas, O. J. D' Souza, S. Detriche, Z. Mekhalif, P. Martis, *Talanta*, 125 (2014) 352.
19. H. Kang, Y. Jin, Q. Han, *Anal. Lett.*, 47 (2014) 1552.
20. J. Sochr, L. Svorc, M. Rievaj, D. Bustin, *Diamond Relat. Mater*., 43 (2014) 5.
21. N. Xiao, B. J. Venton, *Anal. Chem*., 84 (2012) 7816.
22. R. N. Goyal, S. Bushnoi, *Talanta*, 84 (2011) 78.
23. H.-M. Zhang, X.-L. Zhou, R.-T. Hui, N.-Q. Li, D.-P. Liu, *Talanta*, 56 (2002) 1081.
24. S.-F. Wang, D. Du, Q.-C. Zou, *Talanta*, 57 (2002) 687.
25. P. Hernandez, I. Sanchez, F. Paton, L. Hernandez, *Talanta*, 46 (1998) 985.
26. K. Pihel, T. J. Schroeder, R. M. Wightman, *Anal. Chem*., 66 (1994) 4532.
27. S. S. M. Hassan, G. A. Rechnitz, *Anal. Chem*., 58 (1986) 1052.
28. L. Wang, J. Bai, P. Huang, H. Wang, L. Zhang, Y. Zhao, *Int. J. Electrochem. Sci*., 1 (2006) 238.
29. J. Gong, X. Lin, *Electrochim. Acta*, 49 (2004) 4351.
30. E. Dempsey, A. Kennedy, N. Fay, T. McCormac, *Electroanalysis*, 15 (2003) 1835.
31. M. L. A. V. Heien, P. E. M. Phillips, G. D. Stuber, A. T. Seipel, R. M. Wightman, *Analyst*, 128 (2002) 1413.
32. P. Takmakov, M. K. Zachek, R. B. Keithley, P. L. Walsh, C. Donley, G. S. McCarty, R. M. Wightman, *Anal. Chem*., 82 (2010) 2020.
33. B. D. Bath, H. B. Martin, R. M. Wightman, M. R. Anderson, *Langmuir*, 17 (2001) 7032.
34. B. V. Sarada, T. N. Rao, D. A. Tryk, A. Fujishima, *Anal. Chem*., 72 (2000) 1632.
35. Y. Yang, W. Yan, C. Jing, *Langmuir*, 28 (2012) 14588.
36. S. L. Jewett, S. Eggling, L. Geller, *J. Inorg. Biochem*., 66 (1997) 165.
37. C. A. Gorski, M. Aeschbacher, D. Soltermann, A. Voegelin, B. Baeyens, M. M. Fernandes, T. B. Hofstetter, M. Sander, *Environ. Sci. Technol*., 46 (2012) 9360.

38. C. A. Gorski, L. Klupfel, A. Voegelin, M. Sander, T. B. Hofstetter, *Environ. Sci. Technol*., 46 (2012) 9369.
39. H. Yao, Y. Sun, X. Lin, Y. Tang, A. Liu, G. Li, W. Li, S. Zhang, *Anal. Sci*., 23 (2007) 677.
40. L. Zou, Y. Li, S. Cao, B. Ye, *Talanta*, 117 (2013) 333.
41. X. Li, M. Chen, X. Ma, X. Lin, *Int. J. Chem*., 2 (2010) 206.
42. H.-P. Wu, T.-L. Cheng, W.-L. Tseng, *Langmuir*, 23 (2007) 7880.
43. S. Garnayak, S. Patel, *Ind. Eng. Chem. Res*., 53 (2014) 12249.
44. Z. Tao, G. Wang, J. Goodisman, T. Asefa, *Langmuir*, 25 (2009) 10183.
45. J. Wang, Analytical Electrochemistry, John Wiley and Sons Inc., (2006) New Jersey, U. S. A.
46. K. G. Bhattacharyya, S. S. Gupta, *Ind. Eng. Chem. Res*., 45 (2006) 7232.
47. O. Gilbert, B. E. Kumara Swamy, U. Chandra, B. S. Sherigara, *Int. J. Electrochem. Sci*., 4 (2009) 582.
48. A. Fitch, A. Agyeman, A. Wagdy, Z. Terranova, *Langmiur*, 27 (2011) 452.